AFRL-RX-WP-TP-2011-4363

LOAD-DIFFERENTIAL FEATURES FOR AUTOMATED DETECTION OF FATIGUE CRACKS USING GUIDED WAVES (PREPRINT)

Jennifer E. Michaels, Sang Jun Lee, Xin Chen, and Thomas E. Michaels

Georgia Tech Research Group

NOVEMBER 2011

STINFO COPY

AIR FORCE RESEARCH LABORATORY
MATERIALS AND MANUFACTURING DIRECTORATE
WRIGHT-PATTERSON AIR FORCE BASE, OH 45433-7750
AIR FORCE MATERIEL COMMAND
UNITED STATES AIR FORCE

REPORT DOCUMENTATION PAGE

1. REPORT DATE *(DD-MM-YY)*	2. REPORT TYPE	3. DATES COVERED *(From - To)*
November 2011	Technical Paper	1 November 2011 – 1 November 2011

4. TITLE AND SUBTITLE	5a. CONTRACT NUMBER
LOAD-DIFFERENTIAL FEATURES FOR AUTOMATED DETECTION OF FATIGUE CRACKS USING GUIDED WAVES (PREPRINT)	FA8650-09-C-5206

5b. GRANT NUMBER

5c. PROGRAM ELEMENT NUMBER
62102F

6. AUTHOR(S)	5d. PROJECT NUMBER
Jennifer E. Michaels, Sang Jun Lee, Xin Chen, and Thomas E. Michaels	4349

5e. TASK NUMBER
41

5f. WORK UNIT NUMBER
LP106300

7. PERFORMING ORGANIZATION NAME(S) AND ADDRESS(ES)	8. PERFORMING ORGANIZATION REPORT NUMBER
Georgia Tech Research Group 305 10th Street NW Atlanta, GA 30332	

9. SPONSORING/MONITORING AGENCY NAME(S) AND ADDRESS(ES)	10. SPONSORING/MONITORING AGENCY ACRONYM(S)
Air Force Research Laboratory Materials and Manufacturing Directorate Wright-Patterson Air Force Base, OH 45433-7750 Air Force Materiel Command United States Air Force	AFRL/RXLP

11. SPONSORING/MONITORING AGENCY REPORT NUMBER(S)
AFRL-RX-WP-TP-2011-4363

12. DISTRIBUTION/AVAILABILITY STATEMENT
Approved for public release; distribution unlimited.

13. SUPPLEMENTARY NOTES
This work was funded in whole or in part by Department of the Air Force contract FA8650-09-C-5206. The U.S. Government has for itself and others acting on its behalf an unlimited, paid-up, nonexclusive, irrevocable worldwide license to use, modify, reproduce, release, perform, display, or disclose the work by or on behalf of the U.S. Government. PA Case Number and clearance date: 88ABW-2011-4532, 19Aug 2011. Preprint journal article to be submitted to Review of Progress in Quantitative NDE Conference Proceeding. This document contains color.

14. ABSTRACT
Guided wave structural health monitoring (SHM) is being used to assess the integrity of plate-like structures for aerospace, civil and mechanical applications. Prior research has investigated how guided wave propagation is affected by applied loads, which induce anisotropic changes in both dimensions and phase velocity. In addition, it is well-known that applied tensile loads open fatigue cracks and thus enhance their detectability using ultrasonic methods. Here we introduce a class of load-differential methods in which signals recorded from different loads at the same damage state are compared without using previously obtained damage-free data. Changes in delay-and-sum images are considered as a function of differential loads. Load-differential features are extracted from these images that capture the effects of loading as fatigue cracks are opened. Damage detection thresholds are adaptively set based upon the load-differential behavior of the various features, which enables implementation of an automated fatigue crack detection process.

15. SUBJECT TERMS
guided waves, sparse array, load-differential imaging, fatigue crack, feature selection

16. SECURITY CLASSIFICATION OF:			17. LIMITATION OF ABSTRACT:	18. NUMBER OF PAGES	19a. NAME OF RESPONSIBLE PERSON (Monitor)
a. REPORT	b. ABSTRACT	c. THIS PAGE	SAR	10	Charlie Buynak
Unclassified	Unclassified	Unclassified			19b. TELEPHONE NUMBER *(Include Area Code)* N/A

LOAD-DIFFERENTIAL FEATURES FOR AUTOMATED DETECTION OF FATIGUE CRACKS USING GUIDED WAVES

Xin Chen, Sang Jun Lee, Jennifer E. Michaels, and Thomas E. Michaels

School of Electrical and Computer Engineering,
Georgia Institute of Technology, Atlanta, Georgia 30332-0250

ABSTRACT. Guided wave structural health monitoring (SHM) is being used to assess the integrity of plate-like structures for aerospace, civil and mechanical applications. Prior research has investigated how guided wave propagation is affected by applied loads, which induce anisotropic changes in both dimensions and phase velocity. In addition, it is well-known that applied tensile loads open fatigue cracks and thus enhance their detectability using ultrasonic methods. Here we introduce a class of load-differential methods in which signals recorded from different loads at the same damage state are compared without using previously obtained damage-free data. Changes in delay-and-sum images are considered as a function of differential loads. Load-differential features are extracted from these images that capture the effects of loading as fatigue cracks are opened. Damage detection thresholds are adaptively set based upon the load-differential behavior of the various features, which enables implementation of an automated fatigue crack detection process. The efficacy of the proposed approach is examined using data from a fatigue test performed on an aluminum plate specimen that is instrumented with a sparse array of surface-mounted ultrasonic guided wave transducers.

INTRODUCTION

Many structural health monitoring (SHM) methods have focused on aging engineering structures. In particular, ultrasonic guided waves are being proposed to assess the integrity of plate-like structures because of their ability to inspect large scale areas at low cost. Recently, sparse transducer array configurations have been proposed in conjunction with imaging algorithms, which are based upon baseline subtraction for damage detection and localization [1-3]. It is well known that guided waves are sensitive to variable environmental and operational conditions [4-7]. Applied loads are one such operational condition and affect guided wave propagation by inducing anisotropic changes in both specimen dimensions and wave phase velocity. However, applied tensile loads can open fatigue cracks and thus enhance the detectability of guided waves.

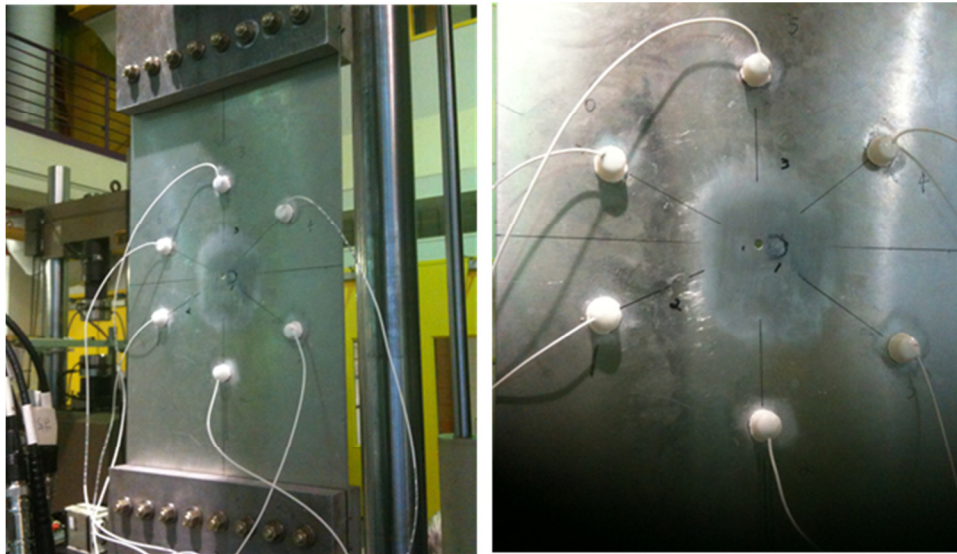Work presented here is based upon constructing a series of load-differential images using the delay-and-sum imaging algorithm. Different features from these images are selected to adaptively determine a threshold for damage detection, which enables an automated process for detection of fatigue cracks. The efficacy of the proposed approach is evaluated using experimental data from a fatigue test.

EXPERIMENTAL SETUP

A fatigue experiment was performed to obtain data from a metallic specimen with growing cracks. A 6061 aluminum plate of 305 mm × 610 mm × 3.18 mm was instrumented with an array of six piezoelectric transducers fabricated from 7 mm diameter, 300 kHz, radial mode PZT discs. The transducers were bonded to the plate with epoxy and subsequently reinforced with a bubble-filled epoxy protection backing. The transducers were excited with a linear chirp excitation sweeping from 50 to 500 kHz with a duration of 0.2 ms. Signals were generated using the NI PXIe-5122 waveform generator and received via the Panametrics 5072PR amplifier. A custom multiplexer was used to switch the 15 unique transmit-receive pairs. The signals were then digitized with the NI PXI-5412 14-bit digitizer at a sampling frequency of 20 MHz, and 20 waveforms were averaged for each acquisition.

By utilizing a broadband chirp excitation, a high signal-to-noise ratio was achieved and multiple guided wave modes were generated in the plate. Signals were filtered to yield the equivalent narrow-band tone burst response by applying filtering in the frequency domain [8]. A 5-cycle tone burst response at 100 kHz was selected because of the purity of A_0 mode and its sensitivity to through-thickness cracks.

The experiment was performed on an MTS servo-hydraulic test machine running in load control mode as shown in Figure 1. After measuring baseline data from the pristine condition of the specimen, a 5.1 mm diameter through-thickness hole was drilled in the center of the specimen, and a small starter notch was introduced in one side of the hole as a site for initialization of crack growth. The plate was fatigued using a sinusoidal tension-tension cycling load ranging from 16.5 to 165 MPa with a frequency of 3 Hz. The entire fatiguing progress is summarized in [9] and Table 1. For each interval throughout fatiguing, ultrasonic data sets were recorded as a function of applied static tensile load from 0 to 115 MPa in steps of 11.5 MPa, for a total of 11 loading values per data set.

FIGURE 1. Aluminum specimen mounted on the MTS machine

TABLE 1. Summary of Fatiguing Schedule and Data Acquired

Data Set	Fatigue Cycles	Notes / Crack Lengths at Surface	
		Left	Right
1	0	Baseline, no hole, no notch	
2	0	5.1 mm diameter hole drilled	
3	0	Starter notch cut (left, front of hole)	
4	5000	No visible cracks	
5	8000	1.65 mm	----
6	10000	3.56 mm	----
7	12500	5.36 mm	----
8	15500	7.65 mm	----
9	17000	9.91 mm	----
10	18500	13.41 mm	4.72 mm
11	19500	16.81 mm	8.43 mm
12	20000	19.46 mm	11.48 mm
13	20400	22.71 mm	15.57 mm
14	20600	25.20 mm	18.75 mm

IMAGING METHOD

The delay-and-sum imaging algorithm is used here to visualize the effect that applied tensile loads can have on opening fatigue cracks. Consider sets of signals recorded at two different static load levels from all transducer pairs under the same damage state. For convenience, we refer to the set recorded at the lower load level as the reference signals and the set recorded at the higher load level as the current signals. Consider sensor pair ij where the ith transducer is the transmitter located at (x_i, y_i), and jth transducer is the receiver located at (x_j, y_j).). If there is a scatterer at (x,y), the delay time that corresponds to the scattered signal path is:

$$t_{xy}^{ij} = \frac{\sqrt{(x_i - x)^2 + (y_i - y)^2} + \sqrt{(x_j - x)^2 + (y_j - y)^2}}{c_g} \tag{1}$$

where the c_g is the group velocity estimated from the times of the first arrivals from all transducer pairs. Let $s_{ij}(t)$ correspond to the differenced signal between the current signal and the reference signal for sensor pair ij. The signal $s_{xy}(t)$ is the sum of the shifted signals scattered from the point (x,y) from all transducer pairs:

$$s_{xy}(t) = \sum_i \sum_j s_{ij}(t - t_{xy}^{ij}). \tag{2}$$

The image value at the pixel (x,y) is calculated as:

$$E_{xy} = \int_{t_1}^{t_2} s_{xy}^2(t)dt, \tag{3}$$

where t_1 and t_2 are the start and end times of the selected time window respectively. Although the differenced signal in Eq. (3) can be either the raw (RF) signal, or the envelope-detected (rectified) signal, here we use only the envelope-detected signals.
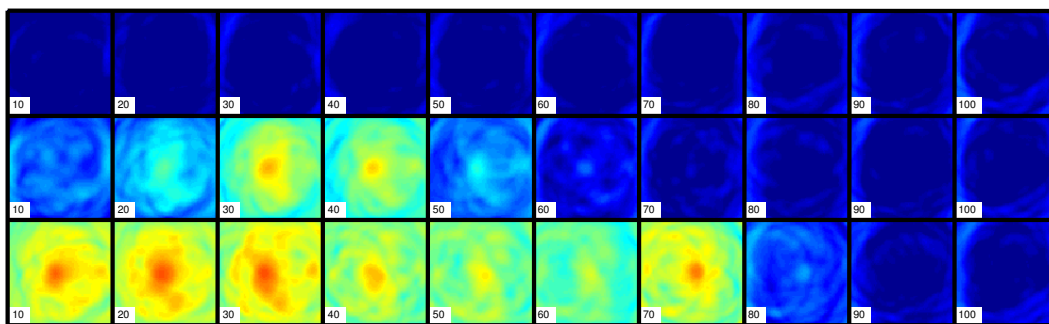
By subtracting two adjacent signals recorded at different loads (e.g., 40% - 30%), ten load-differential signals are obtained per data set for each transducer pair. These signals can be used as the differenced signals in Eq. (2) to generate ten load-differential images per data set, which correspond to differential loads increasing from 0-10% to 90-100%. Figure 2 shows these images for data sets 4, 8 and 11, which correspond to no crack, one crack, and two cracks on each side of the hole. The images clearly indicate that cracks open with loads, and that different cracks open at different load levels.
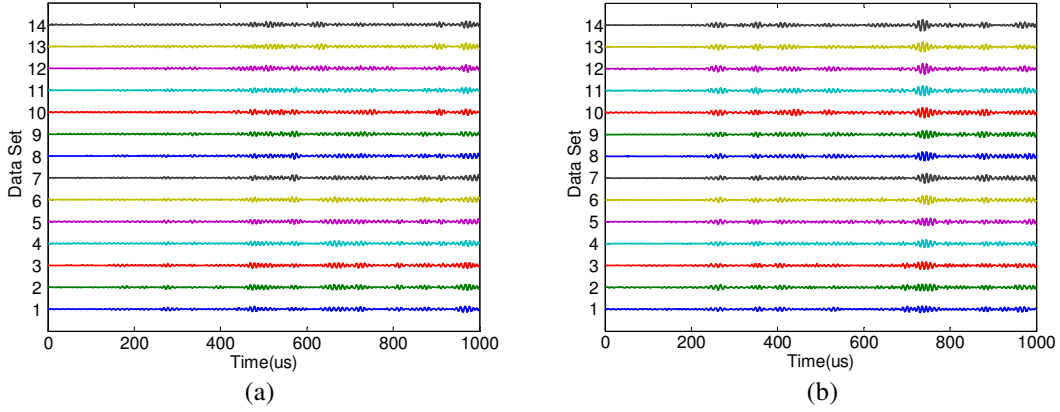
FEATURE SELECTION

Loading Effects at Maximum Load Level

After generating the load-differential images, several features are examined for automated detection of cracks. It is assumed that as the load increases above a certain level, all fatigue cracks are fully opened. Under this assumption, the load-differential signals at maximum load level (100% - 90%) reflect only the loading effects, not crack opening effects. Figure 3(a) shows the load-differential signals at maximum load level for all of the 14 data sets from transducer pair 1-2 (i.e., transmitting on 1 and receiving on 2), where the direct path does not go through the cracked area and thus the signals are less affected by the cracks. Figure 3(b) shows the load-differential signals from transducer pair 2-5, where the direct path does go through the cracks and thus the signals are most affected by the cracks. It is clear in both cases that the load-differential signals at maximum load level are nearly identical in both amplitude and shape for all data sets.

Similarly the load-differential images generated at the maximum load level also assumed only the loading effects since cracks are fully opened. Using images instead of pair-wise signals is advantageous because information from all transducer pairs is incorporated. As shown in Figure 2, the images from the maximum load level have similar image patterns and energy levels. Features of the last load-differential image are used as references for other images from the same data set (i.e., the same damage state) to detect fatigue crack(s).

FIGURE 2. Load-differential images generated from data sets 4, 8 and 11 (top to bottom). The differential loads increase from 0-10% to 90-100% from left to right, and the color scale is 30 dB

FIGURE 3. Load-differential signals at maximum load level (100% -90%) for all 14 datasets. (a) Transducer pair 1-2. (b) Transducer pair 2-5.

Total Energy

The first feature used in this study tracks the energy of the load-differential images as cracks are opened with load. The total energy over the imaged plate area is calculated as:

$$E^k = \sum_i e_{k_i},\qquad(4)$$

where k is the kth load-differential image of each data set $(k = 1,\ldots,K)$ and K is the number of differential loading cases, in our case $K=10$. The variable e_{k_i} is the energy of the ith pixel in the area of interest of the kth image.

The total energy from each differential image is then normalized to that of the last load-differential image (i.e., at maximum load):

$$E^k_{\text{Norm}} = 10\log_{10}\left(\frac{E^k}{E^K}\right).\qquad(5)$$

In order to extract a single value feature and increase the robustness of the algorithm, the mean of normalized total energy value of each data set is calculated as:

$$\bar{E}_{\text{Norm}} = \frac{\sum\limits_{k} E^k_{\text{Norm}}}{K}.\qquad(6)$$

This parameter is used to decide if cracking has occurred for the data set of interest.

2-D Correlation Coefficient

The next feature considered compares the pattern of each image to that of the final image acquired at maximum load. The 2-D correlation coefficient is used to determine the similarity of the images [10]. In contrast to the energy feature, this method tracks the changes in the pattern of the load-differential images that are affected by crack opening effects. As Figure 2 shows, the pattern differences are obvious between the set of images

that include crack opening effects and those that reflect only loading effects. Because a change in pixel energy level of the image does not produce a pattern difference, the correlation coefficient between two signals is evaluated as a damage-sensitive feature. The 2-D correlation coefficient between two images is calculated as:

$$r_k = \frac{\sum_i (e_{k_i} - \overline{e}_k)(e_{K_i} - \overline{e}_K)}{\sqrt{\sum_i (e_{k_i} - \overline{e}_k)^2} \sqrt{\sum_i (e_{K_i} - \overline{e}_K)^2}}, \qquad (7)$$

where the average values $\overline{e}_k$ and $\overline{e}_K$ are defined as:
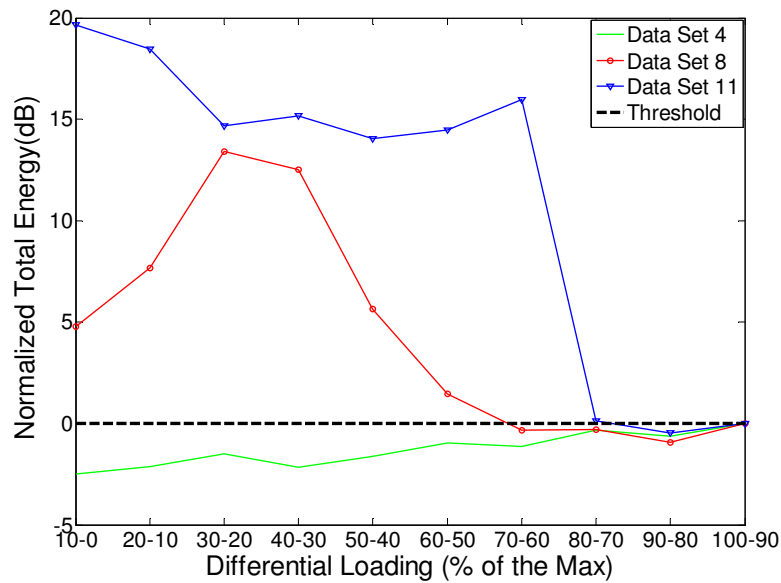
$$\overline{e}_k = \frac{1}{N} \sum_i e_{k_i} \quad \text{and} \quad \overline{e}_K = \frac{1}{N} \sum_i e_{K_i}, \qquad (8)$$

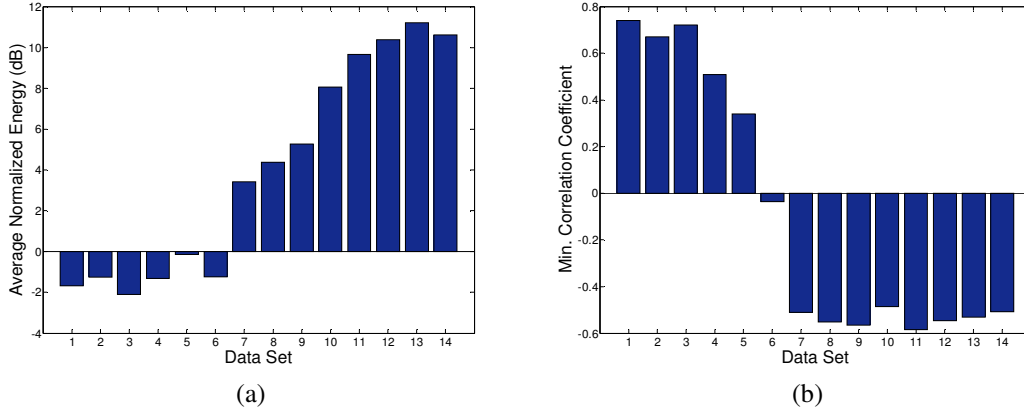respectively and N is the number of pixels in the image.

RESULTS AND DISCUSSION

Figure 4 is the plot of normalized total energy vs. differential loading for data sets 4, 8 and 11. It clearly shows that load-differential images with the crack opening effects have much higher energy values than those with only loading effects. As suggested by Figure 2, if the total energy from the last-differential image of each data set is used as a threshold, all images with the crack opening effects are detected as damaged.

To further simplify the auto-detection process, the mean of normalized total energy values of all 14 data sets are plotted in a bar chart as shown in Figure 5(a). Values above 0 dB indicate the possible existence of fatigue crack(s).

FIGURE 4. Normalized total energy of data sets 4, 8 and 11.

FIGURE 5. Crack auto-detection by two features. (a) The mean of normalized total energy values. (b) The minimum 2-D correlation coefficient values.

The 2-D correlation coefficients are calculated between the last load-differential image and the other images from the same data set and are summarized in Table 2. Negative coefficients indicate significant differences between image patterns, which are further evidence that those images may contain information about crack(s). The minimum correlation coefficient is selected for each data set and plotted in a bar chart as shown in Figure 5(b). Values below 0 dB indicate the possible existence of fatigue crack(s).

As shown in Figure 5, both features offer a potential for automated detection of fatigue crack(s). While the energy feature shows a monotonic increasing trend with the numbers of cracks and their lengths, the 2-D correlation coefficient feature provide a more pronounced indication of cracking. Neither feature is expected to be sensitive to the orientation of cracks.

TABLE 2. Summary of 2-D Correlation Coefficients from All Data Sets

Data Set	2-D Correlation Coefficient (With respect to the last load differential image of every dataset)									
1	0.87	**0.74**	0.85	0.79	0.80	0.85	0.88	0.90	0.91	1
2	**0.67**	0.85	0.78	0.82	0.86	0.82	0.88	0.86	0.93	1
3	0.78	0.77	0.80	**0.72**	0.82	0.86	0.80	0.85	0.83	1
4	**0.51**	0.70	0.81	0.87	0.87	0.87	0.91	0.94	0.91	1
5	**0.34**	0.53	0.73	0.82	0.78	0.87	0.90	0.93	0.94	1
6	0.43	0.32	0.48	0.27	**-0.04**	-0.02	0.68	0.86	0.89	1
7	0.41	0.20	-0.32	-0.49	**-0.51**	-0.46	0.62	0.86	0.91	1
8	0.11	-0.48	**-0.55**	-0.52	-0.35	0.50	0.84	0.88	0.91	1
9	-0.50	**-0.57**	-0.53	-0.38	-0.38	0.25	0.87	0.90	0.91	1
10	**-0.49**	-0.43	-0.35	-0.39	-0.37	-0.33	-0.45	-0.13	0.83	1
11	-0.55	-0.51	-0.50	-0.49	**-0.58**	-0.52	-0.23	0.53	0.90	1
12	-0.51	-0.53	**-0.55**	-0.37	-0.09	-0.01	-0.16	0.57	0.91	1
13	**-0.53**	-0.51	-0.19	-0.22	-0.38	-0.39	-0.33	0.83	0.88	1
14	**-0.51**	-0.25	-0.29	-0.45	-0.51	-0.30	-0.13	0.70	0.81	1

CONCLUSIONS

Load-differential images, which do not require any previously obtained damage-free baseline data, show crack opening effects as a function of load. After applying sufficient loadings to fully open fatigue crack(s), the pair-wise load-differential signals and the delay-and-sum images reflect only the loading effects. It is possible to select features based on this observation to automatically detect the existence of fatigue crack(s). In this paper, two features of the load-differential images, the total energy and the 2-D correlation coefficient, are evaluated. Future work should investigate additional features, selection of optimal thresholds, and more complex specimens.

ACKNOWLEDGEMENTS

REFERENCES

1. J. E. Michaels, A. J. Croxford and P. D. Wilcox, "Imaging algorithms for locating damage via in situ ultrasonic sensors," in *Proc. IEEE Sensors Applications Symposium* (2008), pp. 63-67.
2. J. E. Michaels, "Detection, localization and characterization of damage in plates with an *in situ* array of spatially distributed ultrasonic sensors," *Smart Mater. Struct*., **17**, 035035(15pp) (2008).
3. C. Wang, J. T. Rose, and F.-K. Chang, "A synthetic time-reversal imaging method for structural health monitoring," *Smart Mater. Struct.*, **13**, pp. 415-423 (2004).
4. Y. Lu and J. E. Michaels, "A methodology for structural health monitoring with diffuse ultrasonic waves in the presence of temperature variations," *Ultrasonics*, **43**, pp. 717-731 (2005).
5. G. Konstantinidis, B. W. Drinkwater and P. D. Wilcox "The temperature stability of guided wave structural health monitoring systems," *Smart Mater. Struct.,* **15**, pp. 967-976 (2006).
6. F. Chen and P. D. Wilcox, "The effect of load on guided wave propagation," *Ultrasonics*, **47**, pp.111-122 (2007).
7. J. E. Michaels, S. J. Lee and T. E. Michaels, "Effects of applied loads and temperatures on ultrasonic guided waves," in *Proc. EWSHM*, edited by F. Casciati and M. Giordano, (2010), pp. 1267-1272.
8. J. E. Michaels, S. J. Lee, J. S. Hall and T. E. Michaels, "Multi-mode and multi-frequency guided wave imaging via chirp excitations," in *Proc. SPIE*, **7984**, edited by T. Kundu, (2011), 79840I (11 pp).
9. S. J. Lee, J. E. Michaels, X. Chen, and T. E. Michaels, "Fatigue crack detection via load-differential guided wave methods," in *Review of Progress in QNDE*, **31**, edited by D. O. Thompson and D. E. Chimenti (Eds.), AIP, in press, expected 2012.
10. W. Burger and M. J. Burge, *Principles of Digital Image Processing*, Springer-Verlag, London (2009), pp. 260- 266.